*The Canadian Mineralogist*
Vol. 35, pp. 105-118 (1997)

# ZIRCON- AND MONAZITE-FORMING METAMORPHIC REACTIONS AT MANITOUWADGE, ONTARIO

YUANMING PAN[1]

*Department of Geological Sciences, University of Saskatchewan, Saskatoon, Saskatchewan S7N 5E2*

## ABSTRACT

At the Manitouwadge volcanogenic massive sulfide camp, Ontario, a garnet-rich cordierite–orthoamphibole gneiss and a calc-silicate rock contain an unusually high abundance of zircon, monazite, allanite, fluorapatite, and titanite, and minor amounts of other accessory minerals (xenotime, zirconolite, Zr-bearing rutile, columbite, thorite, bastnäsite and synchysite). The majority of the zircon grains in the garnet-rich cordierite–orthoamphibole gneiss are igneous in origin, and have survived a seafloor hydrothermal alteration and an upper-amphibolite-facies regional metamorphism. Metamorphic zircon occurs mainly at the expense of igneous zircon *via* a reaction such as $(Zr,Hf,Y,REE)(Si,P)O_4 \rightarrow (Zr,Hf)SiO_4 + (Y,REE)PO_4$. The occurrence of metamorphic zircon, titanite and rutile in replacement assemblages after zirconolite is probably related to a reaction such as $CaZrTi_2O_7 + 2Si^{4+} + 4O^{2-} \rightarrow ZrSiO_4 + CaTiSiO_5 + TiO_2$. There are two compositionally distinct types of monazite: Th-rich (3–12 wt% $ThO_2$) and Th-poor (<1.5 wt% $ThO_2$). However, available monazite U–Pb ages (Davis *et al.* 1994) show that both compositional varieties crystallized during the high-grade metamorphism and most likely formed from pre-existing *REE*-rich minerals. In addition, some grains of Th-poor monazite formed during retrograde metamorphism as replacement after metamorphic allanite, fluorapatite, and titanite. This study illustrates the importance of accessory minerals in controlling the crystallization of zircon and monazite during prograde and retrograde metamorphism. Moreover, the robust U–Pb dates obtained from zircon and monazite can be integrated with specific metamorphic P–T estimates from their related accessory minerals, which provides important insights into the tectonic evolution of metamorphic terranes.

*Keywords:* zircon, monazite, accessory minerals, prograde and retrograde metamorphism, metamorphic reactions, U–Pb geochronology, P–T–t path, Manitouwadge, Ontario.

## SOMMAIRE

Dans le camp minier de Manitouwadge, en Ontario, où l'on exploite des amas sulfurés volcanogéniques, un gneiss à cordiérite + orthoamphibole riche en grenat et une roche à calc-silicates contiennent une accumulation anomale de zircon, monazite, allanite, fluorapatite, et titanite, et des quantités moins importantes d'autres minéraux accessoires (xénotime, zirconolite, rutile zirconifère, columbite, thorite, bastnäsite et synchysite). La plupart des cristaux de zircon dans le gneiss grenatifère à cordiérite + orthoamphibole ont une origine ignée, et semblent avoir survécu à l'épisode d'altération hydrothermale marine et au métamorphisme régional qui s'en suivit dans le faciès amphibolite supérieur. Le zircon métamorphique a été formé aux dépens du zircon igné par une réaction comme $(Zr,Hf,Y,TR)(Si,P)O_4 \rightarrow (Zr,Hf)SiO_4 + (Y,TR)PO_4$ (*TR*: terres rares). La présence de zircon, titanite et rutile métamorphiques dans les assemblages en remplacement de la zirconolite serait liée à une réaction du genre $CaZrTi_2O_7 + 2Si^{4+} + 4O^{2-} \rightarrow ZrSiO_4 + CaTiSiO_5 + TiO_2$. Deux types de monazite se distinguent par leur composition: 1) riche en Th (3–12% $ThO_2$ en poids), et 2) pauvre en Th (<1.5% $ThO_2$). Les âges U–Pb disponibles sur la monazite (Davis *et al.* 1994) montrent que les deux variétés ont cristallisé au cours de l'épisode de métamorphisme, probablement aux dépens de minéraux de terres rares pré-existants. De plus, certains des cristaux de monazite pauvres en Th se sont formés au cours du métamorphisme rétrograde, en remplacement de l'allanite, la fluorapatite, et la titanite métamorphiques. Ces résultats démontrent le contrôle que peuvent exercer les minéraux accessoires sur la cristallisation du zircon et de la monazite pendant les épisodes de métamorphisme prograde et rétrograde. De plus, on peut intégrer les résultats robustes de la datation U–Pb du zircon et de la monazite à une reconstruction du métamorphisme en termes de P et T à partir de leur cortège de minéraux accessoires associés, ce qui pourrait bien apporter des renseignements précieux dans une reconstruction de l'évolution tectonique des socles métamorphiques.

*Mots-clés:* zircon, monazite, minéraux accessoires, métamorphisme prograde et retrograde, réactions métamorphiques, géochronologie U–Pb, tracé P–T–t, Manitouwadge, Ontario.

[1] *E-mail address*: yuanming.pan@sask.usask.ca

## INTRODUCTION

Zircon and monazite are the two most widely used minerals in U–Pb geochronological studies, because of their high U/Pb ratio, resistance to Pb loss, high blocking temperatures and chemical inertness (Parrish 1990, Heaman & Parrish 1991). These minerals are becoming increasingly important to determine the timing of metamorphism and deformation in order to constrain the pressure – temperature – time – deformation – fluid (P–T–t–d–f) histories of metamorphic terranes (Gromet 1991, Heaman & Parrish 1991). However, unlike most common metamorphic minerals (*e.g.*, garnet: Mezger *et al.* 1989), the metamorphic reactions responsible for the crystallization of zircon and monazite are poorly understood, because these minerals are almost invariably present in low abundance. This factor has seriously hampered an integration of high-precision U–Pb ages with metamorphic P–T estimates, especially in polymetamorphic and polydeformed terranes.

In a routine petrographic examination of cordierite–orthoamphibole rocks from the Manitouwadge mining camp, Ontario (Fig. 1), I encountered textural evidence for the metamorphic crystallization of zircon after

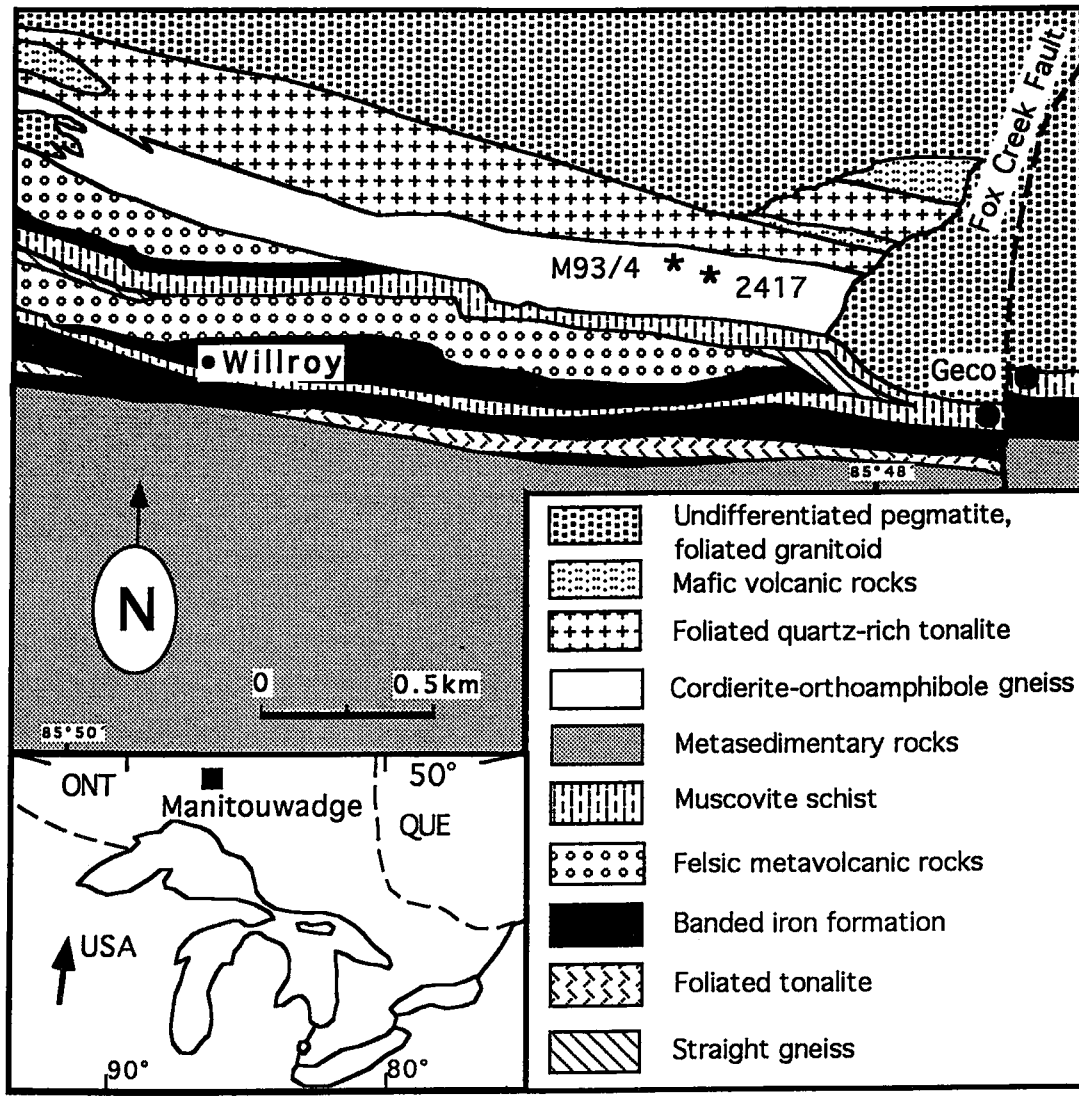


FIG. 1. Simplified geological map of the Willory and Geco mines at Manitouwadge (after Zaleski *et al.* 1994). The location of samples 2417 and M93/4 (garnet-rich cordierite–orthoamphibole gneiss) is shown. Sample 11303 (calc-silicate rock) is from the Geco mine.

pre-existing zirconolite. These cordierite–orthoamphibole rocks and some calc-silicate rocks of the Manitouwadge mining camp examined in previous studies (Pan & Fleet 1992, 1993, 1995) are known to contain unusually high abundances of zircon, monazite, and other exotic accessory minerals (see also Schandl *et al.* 1991, 1995). In addition, the Manitouwadge area has attracted numerous investigators (*e.g.*, Friesen *et al.* 1982, Schandl *et al.* 1991, 1995, Pan & Fleet 1992, 1995, Davis *et al.* 1994, Zaleski & Peterson 1996, Zaleski *et al.* 1994, 1995) because of the occurrence of the large Geco volcanogenic massive sulfide deposit (57 Mt of ore averaging 1.84% Cu, 3.7% Zn and 48 g/t Ag) and three similar but much smaller deposits (Willroy, Willecho and Nama Creek). As a result, the geological history of the Manitouwadge area, including the nature of protoliths, seafloor hydrothermal alteration and regional metamorphism, is reasonably well understood. Moreover, there are a considerable number of high-precision U–Pb dates from zircon, monazite and other accessory minerals for the Manitouwadge area (Table 1). Therefore, the Manitouwadge mining camp provides an opportunity to examine reactions responsible for the crystallization of zircon and monazite during prograde and retrograde metamorphism, and to integrate the metamorphic P–T estimates with available U–Pb zircon and monazite ages to provide constraints on the tectonic evolution of this metamorphic terrane.

TABLE 1. SUMMARY OF GEOCHRONOLOGICAL DATA ON ZIRCON, MONAZITE AND XENOTIME, MANITOUWADGE AREA

U-Pb data from zircon, monazite and xenotime

| Mineral | Rock-type | Comments | Age (Ma) | Ref. |
|---|---|---|---|---|
| zircon | muscovite schist | | 2720±2 | 2 |
| zircon | felsic volcanic suite | | 2722±2 | 3,4 |
| zircon | foliated quartz-rich tonalite | | 2720±3 | 3,4 |
| zircon | metagreywacke | detrital zircon | 2719±2 | 4 |
| zircon | muscovite schist | unabraded | 2703* | 2 |
| zircon | metagreywacke | detrital zircon | 2692±1 | 4 |
| zircon | metagreywacke | detrital zircon | 2679±11 | 4 |
| zircon | K-feldspar porphyritic pluton | | 2680±3 | 3,4 |
| zircon | granite | core | 2682±5 | 5 |
| zircon | granite | brown, prismatic | 2673±4 | 5 |
| monazite | muscovite schist | prismatic | 2675±1 | 1,2 |
| monazite | syn-D1 pegmatite | prismatic | 2669±3 | 3 |
| monazite | syn-D2 tonalite dike | euhedral, prismatic | 2671±3 | 3,4 |
| monazite | pegmatite | euhedral, stubby | 2672±2 | 5 |
| monazite | pegmatite | anhedral | 2673±3 | 5 |
| monazite | granite | stubby | 2672±2 | 5 |
| monazite | granite | clear | 2674±3 | 5 |
| xenotime | granite | | 2669±2 | 5 |
| monazite | biotite schist | cloudy | 2661±1 | 1,2 |
| xenotime | pegmatite | | 2639±2 | 5 |

Single-zircon Pb evaporation data from sample M93/4

| Grain | Description | Evaporation T(°C) | Ages (Ma) |
|---|---|---|---|
| 1 | pale pink, long prismatic | 1580 | 2723±4 |
| | | 1625 | 2731±8 |
| 2 | pale pink, long prismatic | 1585 | 2723±4 |
| | | 1626 | 2743±4 |
| 3 | pale pink, long prismatic | 1628 | 2715±8 |
| 4 | dark brown, anhedral | 1552 | 2703±4 |
| 5 | dark brown, anhedral | 1575 | 2667±8 |
| | | 1608 | 2675±8 |

References: 1, Schandl et al. (1991); 2, Davis et al. (1994); 3, Zaleski et al. (1994); 4, Zaleski et al. (1995); 5, Schandl et al. (1995); * $^{207}Pb/^{206}Pb$ date. Single-zircon Pb evaporation data from Pan & Fleet (1995): zircon grain 2 at 1626°C gave an anomalously old date of 2743±4 Ma.

## GEOLOGICAL SETTING

The Manitouwadge mining camp is located approximately 90 km northeast of Marathon, Ontario, and is situated within the Archean Manitouwadge greenstone belt, along the northern edge of the Wawa Subprovince in the Superior Province. The supracrustal rocks at Manitouwadge consist of a 1- to 2-km-thick sequence of highly deformed and metamorphosed mafic and felsic volcanic and sedimentary rocks, and occur in a reclined, east-northeasterly trending synform (Friesen *et al.* 1982, Zaleski *et al.* 1995). The massive sulfide deposits are hosted by quartz – sillimanite – muscovite schists (Geco mine) and banded iron-formations (Willroy, Willecho and Nama Creek mines), and are characterized by cordierite – orthoamphibole gneisses in the footwall (James *et al.* 1978, Friesen *et al.* 1982, Pan & Fleet 1995). Zircon U–Pb geochronology revealed that the felsic volcanism and associated synvolcanic intrusions occurred at about 2720 Ma (Schandl *et al.* 1991; Davis *et al.*, 1994; Zaleski *et al.* 1994, 1995).

Regional metamorphism at Manitouwadge reached the upper amphibolite facies (James *et al.* 1978, Petersen 1984, Pan & Fleet 1992, Zaleski *et al.* 1994) and was accompanied by extensive anatexis (Robinson 1979, Stevenson & Martin 1986, Zaleski *et al.* 1995). The most comprehensive study on metamorphism at Manitouwadge is that of Petersen (1984), who obtained $650 \pm 30$°C, $6 \pm 1$ kbar, and $a(H_2O) = 0.8 \pm 0.1$ for the upper-amphibolite-facies regional metamorphism. He estimated a temperature of less than 450°C and a pressure of less than 3 kbar for a retrograde event. U–Pb age determinations on metamorphic monazite from the Geco mine (Schandl *et al.* 1991, Davis *et al.* 1994) indicate that the peak regional metamorphism at Manitouwadge occurred at $2675 \pm 1$ Ma. This age is supported by subsequent U–Pb and $^{207}Pb/^{206}Pb$ ages on metamorphic zircon (Schandl *et al.* 1995, Pan & Fleet 1995; Table 1). Davis *et al.* (1994) also obtained a U–Pb age of $2661 \pm 1$ Ma on monazite from a biotite schist at the Geco mine and linked it to a late, localized episode of K-metasomatism (Table 1).

The cordierite – orthoamphibole gneisses at Manitouwadge form a laterally continuous unit, and are bounded by quartz-rich tonalite and amphibolites to the north and quartz – sillimanite – muscovite schist to the south (Fig. 1). The cordierite – orthoamphibole gneisses contain mainly anthophyllite – gedrite (10–50%), cordierite (5–35%), garnet (5–25%), biotite (5–20%), plagioclase (0–10%), and quartz (0–10%; James *et al.* 1978, Petersen 1984, Pan & Fleet 1995). Many other mineral species have been found; they

include staurolite, sillimanite, ilmenite, gahnite, corundum, hercynite, högbomite, nigerite, cassiterite, magnetite, pyrite, pyrrhotite, chalcopyrite, sphalerite, joseite-B, rutile, fluorapatite, fluorite, allanite, zircon, xenotime, and monazite. These cordierite – orthoamphibole gneisses are noteworthy for the widespread occurrence of replacement textures (*e.g.*, cordierite after staurolite) and mineral zonation (*e.g.*, garnet porphyroblasts), especially in some Al-rich enclaves. These features are similar to those documented in other examples of cordierite – orthoamphibole rocks and associated Al-rich enclaves. They record a complex history of metamorphic crystallization (*cf.* Schumacher & Robinson 1987).

## Samples and Analytical Procedures

The three samples examined in this study were used in previous mineralogical and geochemical studies of the Manitouwadge mining camp (Pan & Fleet 1992, 1993, 1995). Two of these (2417 and M93/4) are representative of a garnet-rich variety of the cordierite – orthoamphibole gneisses (Fig. 1; Alldrick 1974, Pan & Fleet 1995). The third sample (11303) is from a concordant variety of calc-silicate rocks from the Geco mine (Pan & Fleet 1992). Zircon was separated from the 60–120 mesh (0.025–0.0125 cm) fraction of sample M93/4 by conventional magnetic and heavy-liquid

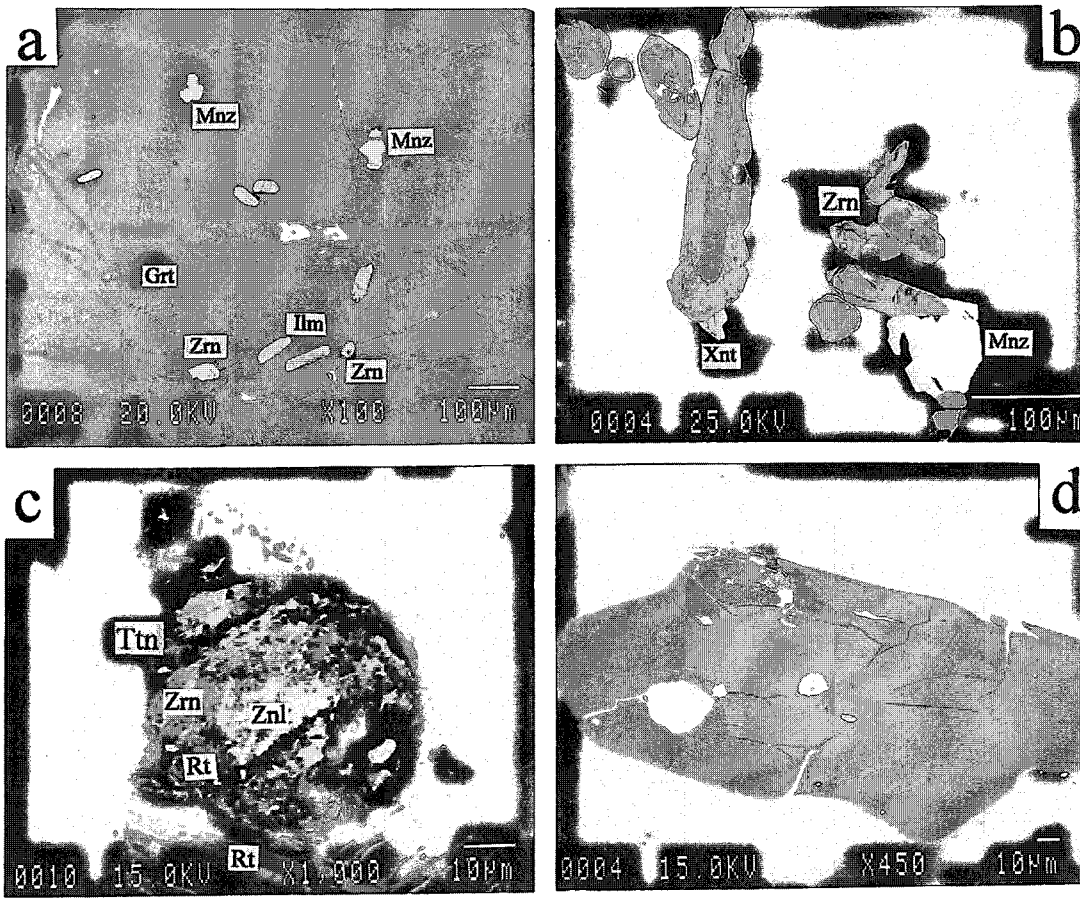


FIG. 2. Back-scattered electron images illustrating the occurrences of zircon and monazite in the garnet-rich cordierite–orthoamphibole gneiss: a) zircon (Zrn), monazite (Mnz) and ilmenite (Ilm) as inclusions in garnet (Grt) porphyroblast; b) zircon in association with xenotime (Xnt) and monazite (Mnz) in cordierite–orthoamphibole–biotite matrix; note the well-developed fractures in the core truncated by less-fractured overgrowth; c) zircon + titanite (Ttn) + rutile (Rt) in replacement assemblage after metamict zirconolite (Znl); d) oscillatory zoning in prismatic zircon; e) metamict zircon with thorite inclusion (Thr) and xenotime along margin; f) cluster of granular monazite partly within a garnet porphyroblast and partly in the matrix; g) oriented monazite inclusions in a porphyroblast of fluorapatite; and h) columbite (white) associated with ilmenite (grey) in gedrite (dark).

methods. Five grains of zircon from sample M93/4 were analyzed for $^{207}Pb/^{206}Pb$ by the modified single-zircon Pb evaporation method of Ansdell & Kyser (1991). Results were reported previously in Pan & Fleet (1995), and are included here in Table 1. The other 452 grains of zircon in M93/4 were first measured for elongation (length/width ratio) and were then mounted in a plug and polished for further petrographic observations and quantitative chemical analyses.

Petrographic observations were made on polished thin sections and grain mounts by a combination of optical microscopy and back-scattered electron imaging obtained on a JEOL–JXA 8600 electron microprobe. Quantitative chemical analyses of minerals were made on that microprobe according to the procedures of Pan & Fleet (1990). Operating conditions included an accelerating voltage of 20 kV, a beam current of 10 nA, a beam diameter of 5 μm, and a counting time of 30 s [except 50 s for rare-earth elements (*REE*) and Y]. Minerals (fluorapatite for P; bustamite, Ca and Mn; diopside, Mg; jadeite, Na; kaersutite, Al and Fe; phlogopite, F; quartz, Si; rutile, Ti; tugtupite, Cl; zircon, Hf and Zr), metals (Th, U, Nb and Ta), and synthetic Y and *REE* phosphates were used as standards.

## Petrography and Mineral Chemistry

### *Garnet-rich cordierite – orthoamphibole gneiss*

The garnet-rich cordierite – orthoamphibole gneiss occurs as a discordant band within the cordierite – orthoamphibole gneisses in the footwall of the Willroy mine (Alldrick 1974, Pan & Fleet 1995). This garnet-rich variety is similar to the host cordierite – orthoamphibole gneisses in major mineral constituents, but is characterized by abundant accessory minerals, including zircon, monazite, xenotime, fluorapatite (Pan & Fleet 1995), and other species (columbite, rutile, zirconolite, thorite, and synchysite).

Zircon in the garnet-rich cordierite – orthoamphibole gneiss occurs most commonly as discrete grains in the matrix of cordierite, anthophyllite – gedrite and biotite, but it also is found as inclusions in garnet porphyroblasts (Fig. 2a). Zircon in the matrix is usually closely associated with xenotime and monazite (Fig. 2b). In sample 2417, zircon has also been observed in association with titanite and rutile in replacement assemblages after metamict zirconolite (Fig. 2c). Nearly all zircon grains in sample M93/4 are pale pink to light brownish

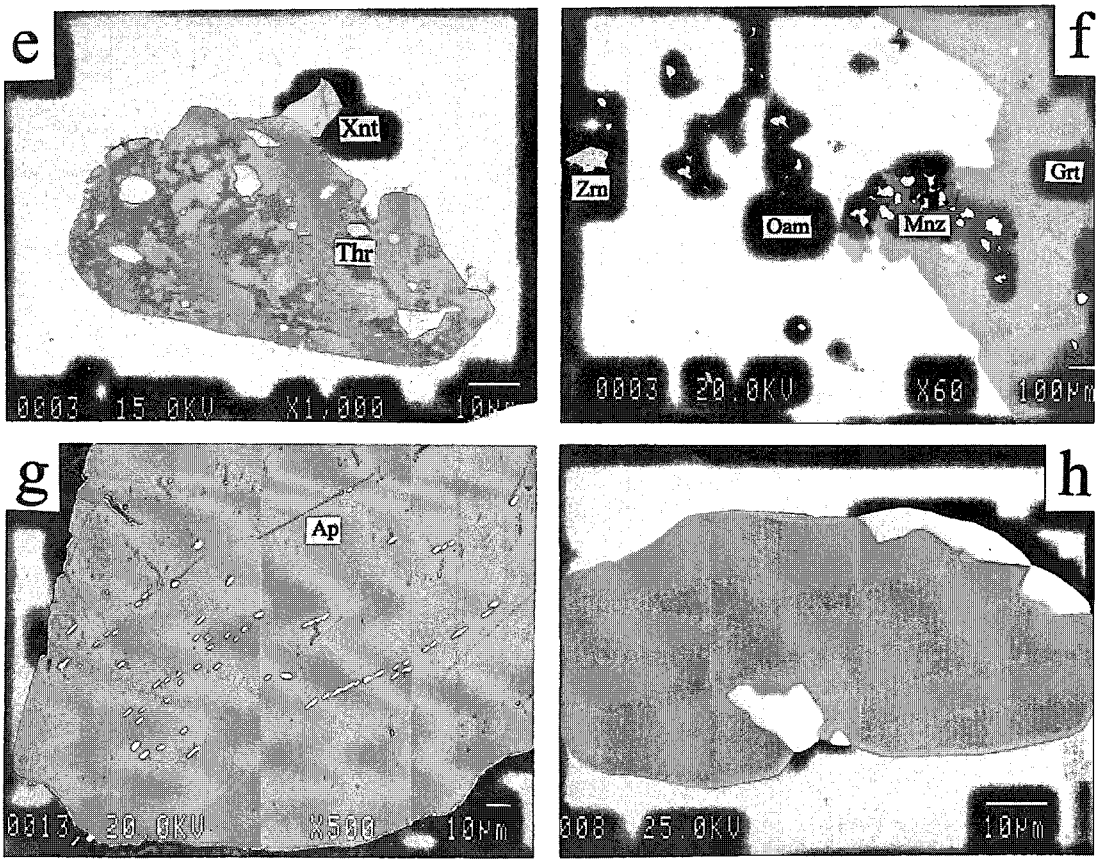

TABLE 2. COMPOSITIONS OF ZIRCON, MONAZITE AND ASSOCIATED ACCESSORY MINERALS IN GARNET-RICH CORDIERITE-ORTHOAMPHIBOLE GNEISS (2417 AND M93/4)

| Mineral | Zircon | | | | | | Monazite | | | | | |
|---|---|---|---|---|---|---|---|---|---|---|---|---|
| Sample | 2417 | | | M93/4 | | | 2417 | | | M93/4 | | |
| Description | clear core | clear zoned | brown margin | clear core | clear zoned | brown grain | granular in matrix | granular in matrix | prismatic in garnet | prismatic inclusion in matrix | granular in apatite | granular in garnet |
| $P_2O_5$ (wt%) | 0.05 | 2.31 | 0 | 0.06 | 1.62 | 0 | 28.4 | 27.9 | 28.8 | 27.5 | 30.0 | 28.4 |
| $Nb_2O_5$ | nd | nd | nd | nd | nd | nd | nd | nd | nd | nd | nd | nd |
| $Ta_2O_5$ | nd | nd | nd | nd | nd | nd | nd | nd | nd | nd | nd | nd |
| $SiO_2$ | 33.1 | 30.1 | 31.3 | 32.6 | 30.8 | 31.1 | 0.08 | 0.33 | 0.66 | nd | nd | nd |
| $TiO_2$ | nd | nd | nd | nd | nd | nd | 0 | 0 | 0 | nd | nd | nd |
| $ZrO_2$ | 65.8 | 61.5 | 66.5 | 66.0 | 62.9 | 66.4 | 0 | 0 | 0 | 0 | 0 | 0 |
| $HfO_2$ | 1.32 | 1.42 | 1.89 | 1.13 | 1.23 | 2.15 | 0 | 0 | 0 | 0 | 0 | 0 |
| $ThO_2$ | nd | nd | nd | nd | nd | nd | 1.16 | 4.50 | 7.99 | 12.5 | 0.88 | 7.52 |
| $U_3O_8$ | nd | nd | nd | nd | nd | nd | 0.22 | 0.13 | 0.22 | 0.29 | 0.32 | 0.42 |
| $Al_2O_3$ | nd | nd | nd | nd | nd | nd | 0 | 0 | 0 | 0 | 0 | 0 |
| $Fe_2O_3$ | 0.10 | 0.08 | 0.40 | 0.26 | 0.29 | 0.54 | 0 | 0.56 | 0.39 | 0.45 | 0 | 0.32 |
| $Y_2O_3$ | 0.38 | 3.48 | 0.04 | 0.21 | 2.15 | 0.02 | 2.38 | 1.64 | 1.75 | 0.68 | 2.16 | 1.98 |
| $La_2O_3$ | 0 | 0 | 0 | 0 | 0 | 0 | 12.1 | 10.3 | 8.91 | 8.44 | 9.21 | 8.34 |
| $Ce_2O_3$ | 0 | 0 | 0 | 0 | 0 | 0 | 30.5 | 26.1 | 24.0 | 22.7 | 26.5 | 25.7 |
| $Pr_2O_3$ | 0 | 0 | 0 | 0 | 0 | 0 | 4.04 | 2.80 | 3.55 | 3.32 | 3.23 | 3.54 |
| $Nd_2O_3$ | 0 | 0.05 | 0 | 0 | 0 | 0 | 15.5 | 15.1 | 14.7 | 14.0 | 16.8 | 14.8 |
| $Sm_2O_3$ | 0 | 0.03 | 0 | 0 | 0 | 0 | 3.35 | 3.9 | 3.06 | 4.05 | 3.99 | 3.56 |
| $Eu_2O_3$ | 0 | 0 | 0 | 0 | 0 | 0 | 0 | 0 | 0 | 0.30 | 0.31 | 0.25 |
| $Gd_2O_3$ | 0.05 | 0.32 | 0 | 0 | 0.21 | 0 | 2.48 | 2.92 | 3.04 | 2.60 | 3.02 | 2.87 |
| $Dy_2O_3$ | 0.07 | 0.53 | 0 | 0.02 | 0.42 | 0 | 0.60 | 0.60 | 0.55 | 0.62 | 0.92 | 0.74 |
| $Er_2O_3$ | 0.06 | 0.42 | 0.03 | 0.05 | 0.25 | 0.02 | 0 | 0 | 0 | 0 | 0 | 0 |
| $Yb_2O_3$ | 0.07 | 0.39 | 0.07 | 0.12 | 0.19 | 0.04 | 0 | 0 | 0 | 0 | 0 | 0 |
| $Lu_2O_3$ | 0 | 0.07 | 0 | 0.02 | 0.03 | 0 | 0 | 0 | 0 | 0 | 0 | 0 |
| CaO | nd | nd | nd | nd | nd | nd | 0.37 | 1.00 | 2.21 | 2.65 | 0.47 | 2.02 |
| $Na_2O$ | nd | nd | nd | nd | nd | nd | 0 | 0 | 0 | 0 | 0 | 0 |
| Total | 101.0 | 100.5 | 100.2 | 100.2 | 100.2 | 100.3 | 98.2 | 100.2 | 99.2 | 99.9 | 97.8 | 100.5 |

in color and have a euhedral to subhedral, prismatic habit. The remaining few are dark brown in color and anhedral in shape. The pale pink to light brownish color of the prismatic zircon, varying significantly in elongation from 1.2 to 8 but peaking in the range 2 to 4 (82%), results from a thin, brownish overgrowth on a clear core, particularly evident in back-scattered electron images (Fig. 2b). Extensive fractures are present in the clear core and are commonly truncated by the unfractured or less highly fractured overgrowth (Fig. 2b). Also, various types of zoning (mainly oscillatory; Fig. 2d) have been observed in the clear core, whereas the brownish overgrowth seems to be more homogeneous. The overgrowth varies significantly in width. A small clear core has also been observed in some of the dark brown grains of zircon. Nine grains of zircon contain thorite inclusions and exhibit extensive metamictization (Fig. 2e).

All grains of zircon in the garnet-rich cordierite–orthoamphibole gneiss are characterized by minor amounts of Hf, Y and heavy *REE* (Table 2). Although the clear core in most zircon grains has less than 0.5 wt% $Y_2O_3$ and 0.5 wt% total $REE_2O_3$, some bands in crystals with oscillatory zoning contain up to 3.5 wt% $Y_2O_3$, 1.8 wt% total $REE_2O_3$ and 2.3 wt% $P_2O_5$ (Table 2). The brownish overgrowth is conspicuously richer in Hf but poorer in Y (and probably *REE* as well) than the clear core (Table 2). The dark brown grains of zircon also are characterized by low levels of Y and *REE*, similar to the brownish overgrowth. An attempt to quantitatively determine the *REE* contents in the clear core and brownish overgrowth of zircon by laser ablation – inductively coupled plasma – mass

TABLE 2 (cont.)

| Mineral | Zirconolite | | Rutile | Xenotime | | Titanite | Columbite | Thorite | Synchysite |
|---|---|---|---|---|---|---|---|---|---|
| Sample | 2417 | | 2417 | 2417 | | 2417 | 2417 | 2417 | M93/4 |
| Description | | | | in matrix | after zircon | | | | |
| $P_2O_5$ (wt%) | 0.12 | 0.05 | 0 | 32.7 | 34.5 | 0 | nd | 0 | nd |
| $Nb_2O_5$ | 1.43 | 4.63 | 1.36 | nd | nd | 0.78 | 73.3 | nd | nd |
| $Ta_2O_5$ | 0.25 | 1.23 | 0 | nd | nd | 0 | 2.36 | nd | nd |
| $SiO_2$ | 0.16 | 0.18 | 0 | 0.11 | 0.15 | 30.5 | nd | 18.1 | 0.73 |
| $TiO_2$ | 35.4 | 31.2 | 94.2 | 0 | 0 | 34.5 | 4.15 | 0 | 0.11 |
| $ZrO_2$ | 35.6 | 34.2 | 1.24 | nd | 0 | nd | 0 | 2.36 | 0 |
| $HfO_2$ | 0.56 | 0.42 | 0.12 | nd | 0 | nd | 0 | 0.05 | 0 |
| $ThO_2$ | 0.15 | 0.11 | 0 | 0 | 0 | nd | 0 | 75.6 | 0 |
| $U_3O_8$ | 0.08 | 0.02 | 0 | 0 | 0 | nd | nd | 1.35 | 0.77 |
| $Al_2O_3$ | 0.45 | 1.23 | 0 | 0 | 0 | 1.88 | nd | 0 | 0 |
| $Fe_2O_3$ | 4.56 | 5.76 | 1.12 | 0.19 | 0.35 | 1.40 | 19.4 | 0.25 | 1.83 |
| $Y_2O_3$ | 2.31 | 1.85 | 0.15 | 40.1 | 45.8 | 0.15 | nd | 0.62 | 1.93 |
| $La_2O_3$ | 0.47 | 0.36 | 0 | 0 | 0 | 0.04 | nd | 0 | 9.44 |
| $Ce_2O_3$ | 1.32 | 1.22 | 0 | 0 | 0 | 0.14 | nd | 0 | 20.4 |
| $Pr_2O_3$ | 0.19 | 0.15 | 0 | 0 | 0 | 0 | nd | 0 | 3.09 |
| $Nd_2O_3$ | 0.78 | 0.66 | 0 | 0.26 | 0 | 0.09 | nd | 0 | 13.5 |
| $Sm_2O_3$ | 0.28 | 0.21 | 0 | 0.47 | 0 | 0.02 | nd | 0 | 2.39 |
| $Eu_2O_3$ | 0 | 0 | 0 | 0.93 | 0.56 | 0 | nd | 0 | 0 |
| $Gd_2O_3$ | 0.46 | 0.35 | 0 | 6.75 | 5.06 | 0 | nd | 0 | 1.40 |
| $Dy_2O_3$ | 0.47 | 0.42 | 0 | 8.29 | 6.79 | 0 | nd | 0 | 0 |
| $Er_2O_3$ | 0.26 | 0.21 | 0 | 5.18 | 2.97 | 0 | nd | 0 | 0 |
| $Yb_2O_3$ | 0.28 | 0.22 | 0 | 3.94 | 2.00 | 0 | nd | 0 | 0 |
| $Lu_2O_3$ | 0 | 0 | 0 | 0.48 | 0.39 | 0 | nd | 0 | 0 |
| CaO | 12.2 | 11.6 | nd | 0 | 0 | 27.3 | nd | 0 | 18.1 |
| $Na_2O$ | 0.12 | 0.11 | nd | 0 | 0 | 0 | nd | 0 | 0.77 |
| F | nd | nd | nd | nd | nd | 0.65 | nd | nd | 5.57 |
| O=F | | | | | | 0.27 | | | 2.35 |
| Total | 97.9 | 96.5 | 98.2 | 99.5 | 98.5 | 97.2 | 99.2 | 98.3 | 72.1 |

wt%, weight percent; nd, not determined; analytical procedures and peak-overlap corrections for REE following those of Roeder (1985) and Pan & Fleet (1990).

spectrometry (*cf.* Fedorowich *et al.* 1995) was not successful owing to the very small grain-size and presence of *REE*-rich mineral inclusions.

Monazite in the garnet-rich cordierite–orthoamphibole gneiss occurs most commonly as inclusions in biotite (see also Schandl *et al.* 1991), but has also been

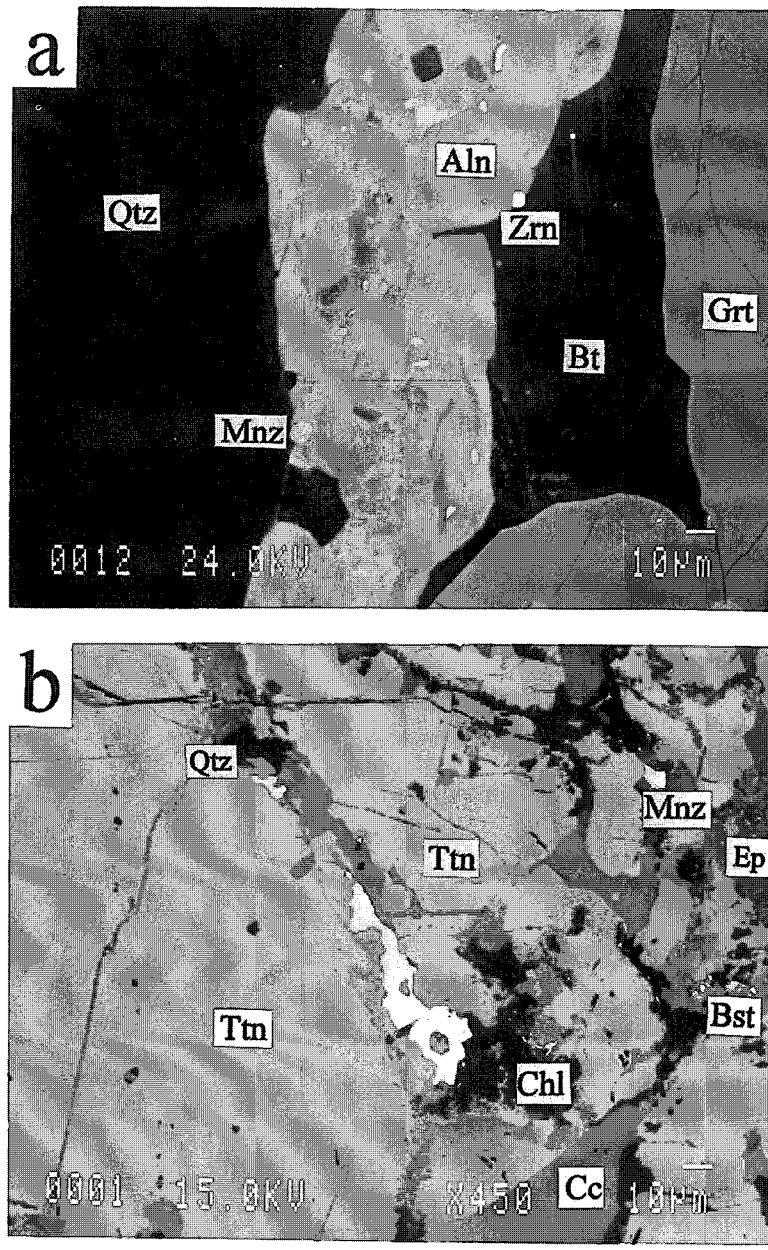


FIG. 3. Back-scattered electron images illustrating the occurrences of zircon and monazite in the calc-silicate rock: a) zircon (Zrn) and monazite (Mnz) associated with a metamict allanite grain (Aln) and other minerals: biotite (Bt), quartz (Qtz), and garnet (Grt); b) monazite (Mnz) associated with calcite (Cc), quartz (Qtz), epidote (Ep), chlorite (Chl), bastnäsite (Bst), and rutile along fractures of titanite (Ttn). Note that the area adjacent to the monazite is darker and has lower levels of *REE* than the area away from it (Table 3; see also Pan *et al.* 1993b).

TABLE 3. COMPOSITIONS OF ZIRCON, MONAZITE AND OTHER ACCESSORY MINERALS IN THE CALC-SILICATE ROCK (11303)

| Mineral | Zircon | | Monazite | | Allanite | | Epidote | | Titanite | | Bastnäsite |
|---|---|---|---|---|---|---|---|---|---|---|---|
| $P_2O_5$ (wt%) | 0 | 0† | 27.5 | 27.9† | nd | nd | nd | nd | nd†† | nd | |
| $Nb_2O_5$ | nd | nd | nd | nd | nd | nd | nd | nd | nd | nd | |
| $Ta_2O_5$ | nd | nd | nd | nd | nd | nd | nd | nd | nd | nd | |
| $SiO_2$ | 32.2 | 31.4 | nd | nd | 35.5 | 33.1 | 38.3 | 30.4 | 30.5 | 0.11 | |
| $TiO_2$ | nd | nd | nd | nd | 0.25 | 0.24 | 0.15 | 35.8 | 34.4 | 0 | |
| $ZrO_2$ | 65.2 | 62.8 | nd | nd | 0.32 | 0.36 | 0 | 0 | 0 | 0 | |
| $HfO_2$ | 1.69 | 1.97 | nd | nd | 0 | 0 | 0 | 0 | 0 | 0 | |
| $ThO_2$ | 0 | 0 | 3.15 | 0.73 | 0 | 0 | 0 | 0 | 0 | 0 | |
| $U_3O_8$ | 0 | 0 | 0 | 0.04 | 0 | 0 | 0 | 0 | 0 | 0 | |
| $Al_2O_3$ | 0 | 0 | 0 | 0 | 21.4 | 18.1 | 24.3 | 1.35 | 1.24 | 0 | |
| FeO | 0.49 | 0.54 | 0 | 0 | 11.2 | 10.58 | 11.2 | 1.63 | 1.45 | 0.45 | |
| MgO | 0 | 0 | nd | nd | 0.12 | 0 | 0 | 0 | 0 | 0 | |
| MnO | 0.43 | 0.36 | nd | nd | 0.45 | 0.84 | 0.70 | 0.23 | 0.21 | 0.18 | |
| $Y_2O_3$ | 0.21 | 0.25 | 1.95 | 2.4 | 0.08 | 0.12 | 0 | 0.45 | 0.08 | 1.24 | |
| $La_2O_3$ | 0 | 0 | 11.3 | 11.1 | 1.31 | 3.70 | 0 | 0 | 0 | 23.5 | |
| $Ce_2O_3$ | 0 | 0 | 29.6 | 29.3 | 3.81 | 9.21 | 0 | 0.22 | 0.05 | 32.1 | |
| $Pr_2O_3$ | 0 | 0 | 3.0 | 3.95 | 0.42 | 1.10 | 0 | 0 | 0 | 3.01 | |
| $Nd_2O_3$ | 0 | 0 | 14.8 | 16.9 | 1.89 | 4.95 | 0 | 0.15 | 0.03 | 10.1 | |
| $Sm_2O_3$ | 0 | 0 | 3.32 | 3.58 | 0.11 | 0.34 | 0 | 0 | 0 | 0.35 | |
| $Eu_2O_3$ | 0 | 0.04 | 0.25 | 0.51 | 0 | 0 | 0 | 0 | 0 | 0 | |
| $Gd_2O_3$ | 0.08 | 0.05 | 2.42 | 2.75 | 0 | 0 | 0 | 0 | 0 | 0 | |
| $Dy_2O_3$ | 0.08 | 0.08 | 0.52 | 0.70 | 0 | 0 | 0 | 0 | 0 | 0 | |
| $Er_2O_3$ | 0.06 | 0.08 | 0.12 | 0 | 0 | 0 | 0 | 0 | 0 | 0 | |
| $Yb_2O_3$ | 0.02 | 0.01 | 0 | 0 | 0 | 0 | 0 | 0 | 0 | 0 | |
| $Lu_2O_3$ | 0 | 0 | 0 | 0 | 0 | 0 | 0 | 0 | 0 | 0 | |
| CaO | 0 | 0 | 0.94 | 0.10 | 19.5 | 14.5 | 22.5 | 27.5 | 27.1 | 1.12 | |
| $Na_2O$ | 0 | 0 | 0 | 0 | 0.12 | 0.22 | 0 | 0.12 | 0 | 0 | |
| F | nd | nd | nd | nd | 0.24 | 0 | 0 | 0.45 | 0.21 | 7.89 | |
| Cl | nd | nd | nd | nd | 0.25 | 0.52 | 0 | 0 | 0 | 0 | |
| O=FCl | | | | | 0.16 | 0.12 | | 0.19 | 0.09 | 3.32 | |
| Total | 100.5 | 97.5 | 98.9 | 99.9 | 96.8 | 96.8 | 97.2 | 98.2 | 95.2 | 76.7 | |

wt%, weight percent; nd, not determined; †, zircon and monazite after allanite; ††, area of titanite adjacent to monazite grains.

observed as prismatic and anhedral granular inclusions in garnet porphyroblasts (Fig. 1a). Although prismatic grains of monazite in the matrix generally occur as discrete grains, clusters of anhedral grains are also common (Fig. 1f). Electron-microprobe analyses reveal that monazite exhibits a bimodal distribution with respect to its Th content: Th-rich (3–12 wt% $ThO_2$) and Th-poor (<1.5 wt%). Both morphological varieties of monazite inclusions in garnet porphyroblasts are Th-rich in composition (>3.75 wt% $ThO_2$), although the highest Th contents (8–12 wt% $ThO_2$) are restricted to the large prismatic grains. Monazite grains in the matrix are either a Th-rich variety (commonly exhibiting a gradual decrease in Th from core to margin, occasionally with a Th-poor rim) or a homogeneous Th-poor one. In addition, monazite has been observed as small rods along the $\{10\bar{1}0\}$ cleavage in fluorapatite porphyroblasts (Fig. 1g) and is invariably the Th-poor variety (<1 wt% $ThO_2$; Table 2).

Measured compositions of the metamict zirconolite conform closely to the ideal formula of $CaZrTi_2O_7$ (Bayliss *et al.* 1989), and are characterized by high Nb contents (up to 4.6 wt% $Nb_2O_5$; Table 2). Rutile in the garnet-rich cordierite–orthoamphibole gneiss contains 1.24 wt% $ZrO_2$ and 1.36 wt% $Nb_2O_5$ (Table 2). Analyses have also been made on rutile in two samples of the host cordierite–orthoamphibole gneisses, but did not reveal any detectable Zr or Nb. Petersen (1984) reported on Sn–Nb-bearing rutile (2.9 wt% $SnO_2$, 3.99 wt% $Nb_2O_5$) in coexistence with cassiterite at the Geco mine, but he did not report Zr. Titanite contains up to 2 wt% $Al_2O_3$, 1.5 wt% $Fe_2O_3$ and 0.9 wt% $Nb_2O_5$. Columbite associated with ilmenite (Fig. 1h) contains minor amounts of Ta and Ti (Table 2). Grains of xenotime associated with zircon and in the matrix are compositionally indistinguishable, and are characterized by high concentrations of the middle *REE* (Table 2). The sole occurrence of synchysite [$Ca(REE)(CO_3)_2F$] in the garnet-rich cordierite–orthoamphibole gneiss is in a cross-cutting quartz – fluorite – fluorapatite vein.

### *Calc-silicate rock*

The calc-silicate rock (sample 11303) is composed of mainly clinopyroxene, garnet and calcic amphiboles (hornblende and actinolite), and minor amounts of plagioclase, quartz, ilmenite, pyrite, titanite, members of the *REE*-bearing epidote–allanite series (referred to as allanite hereafter), zircon and monazite. Both allanite and titanite are apparently in textural equilibrium with garnet and clinopyroxene, as indicated by mutual contacts, and are characterized by varying degrees of metamictization and extensive alteration along grain boundaries and fractures. Zircon and monazite occur as two distinct types: large, discrete grains (50–430 μm in maximum dimension) in direct association with clinopyroxene and garnet, and minute grains (typically less than 5 μm in diameter) in replacement assemblages after metamict allanite and titanite (Fig. 3). Compositions of zircon, monazite, allanite, titanite, epidote, and bastnäsite in the calc-silicate rock are given in Table 3. The allanite is a halogen-bearing variety (Pan & Fleet 1992) and contains a minor amount of Zr (up to 0.36 wt% $ZrO_2$; Table 3). Titanite contains a minor amount of Al, Fe and F, and has detectable *REE*. The zircon after allanite has a low oxide total, probably related to either difficulties in analyzing these very small grains or the presence of water. Monazite in replacement assemblages after titanite and allanite is invariably a Th-poor variety (<1 wt% $ThO_2$; Table 3). The composition of bastnäsite conforms closely to its ideal formula [$(REE)(CO_3)F$].

## Discussion

There is a general consensus that the majority of the cordierite–orthoamphibole gneisses at Manitouwadge originated from tholeiitic basalts *via* seafloor hydrothermal alteration and upper-amphibolite-facies regional metamorphism (James *et al.* 1978, Pan & Fleet 1995, Schandl *et al.* 1995). On the basis of field occurrence, unique geochemistry (high Y, Zr, and *REE*, low $TiO_2$ contents) and single-zircon $^{207}Pb/^{206}Pb$ dates, Pan & Fleet (1995) suggested that the garnet-rich cordierite–orthoamphibole gneiss most likely represents a synvolcanic felsic dike that has undergone the same seafloor hydrothermal alteration and high-grade metamorphism. Pan & Fleet (1992) suggested that the concordant calc-silicate rocks at Manitouwadge represent metamorphosed Ca-rich assemblages that were originally precipitated from Ca-enriched fluids that resulted from interaction with volcanic rocks during seafloor hydrother-

mal alteration (see also Schandl *et al.* 1995). If our interpretations are correct, the garnet-rich cordierite–orthoamphibole gneiss and the calc-silicate rock of this study both have experienced seafloor hydrothermal alteration and upper-amphibolite-facies metamorphism. In addition, most rocks of the Manitouwadge area have undergone retrograde changes (Petersen 1984, Pan & Fleet 1992). The characteristic retrograde assemblages in the cordierite–orthoamphibole gneisses and muscovite schists include andalusite, zoisite, margarite, quartz and plagioclase (Petersen 1984). Pan & Fleet (1992) reported a retrograde assemblage of muscovite, biotite, chlorite, actinolite, and quartz in the calc-silicate rocks of the Geco mine.

*Formation of metamorphic zircon*

The pale pink to light brownish, prismatic grains of zircon have an elongation of mainly 2–4 and as high as 8 (Poldervaart 1956), and $^{207}Pb/^{206}Pb$ ages of about 2720 Ma (Table 1), indicating that they grew during igneous crystallization. These crystals of igneous zircon survived seafloor hydrothermal alteration and upper-amphibolite-facies metamorphism, although a metamorphic overgrowth is almost invariably present (see below). Davis *et al.* (1994) obtained a U–Pb age of 2720 ± 2 Ma on zircon from muscovite schist of the Geco mine (interpreted to represent altered and metamorphosed rhyolites) and confirmed the survival of igneous zircon there. The common occurrences of fractures in igneous zircon (Fig. 2b) may be attributable to intense deformation prior to the high-grade metamorphism or to decay processes (Chakoumakos *et al.* 1987).

The $^{207}Pb/^{206}Pb$ data from dark brown, anhedral grains (Table 1), which are chemically similar to the brownish overgrowths, show that zircon also crystallized during the upper-amphibolite-facies metamorphism. This is supported by the U–Pb age of 2673 ± 4 Ma on a brownish zircon from a granite of the Geco mine (Schandl *et al.* 1995).

The formation of an overgrowth is not uncommon in zircon from high-grade metamorphic rocks (Gupta & Johannes 1985, Vavra *et al.* 1996). Vavra *et al.* (1996) suggested that such a metamorphic overgrowth in granulite-facies metasedimentary rocks formed by addition of Zr from the decomposition of major silicates (*e.g.*, biotite) during anatectic melting. Pidgeon (1992) suggested that solid-state recrystallization of pre-existing (oscillatory zoned) zircon during high-grade metamorphism is most likely responsible for overgrowth in granulites. The occurrence of a metamorphic overgrowth and its common association with xenotime (Fig. 1b) on igneous zircon at Manitouwadge suggests a partial replacement–recrystallization reaction such as:

$$\underset{\text{igneous zircon}}{(Zr,Hf,Y,REE)(Si,P)O_4} \rightarrow \underset{\text{metamorphic zircon}}{(Zr,Hf)SiO_4} + \underset{\text{xenotime}}{(Y,REE)PO_4} \quad (1)$$

The amount of xenotime produced is dependent upon the Y and *REE* contents in igneous zircon. This reaction is consistent with the increase of Hf and a decrease in Y and *REE* from the igneous core to the metamorphic overgrowth (Table 2). Vavra *et al.* (1996) reported a similar distribution of Hf, Y and *REE* between detrital zircon and its metamorphic overgrowth in granulite-facies metasedimentary rocks. Pidgeon (1992) also documented a depletion of U, Th, and Pb during metamorphic recrystallization of pre-existing zircon. At the Geco mine, Schandl *et al.* (1995) obtained a U–Pb date of 2669 ± 2 Ma on a clear grain of xenotime in a granite (Table 1), also consistent with its crystallization during high-grade metamorphism.

The presence of zircon, titanite and rutile in replacement assemblages after zirconolite (Fig. 2c) is probably related to the following reaction:

$$CaZrTi_2O_7 + 2Si^{4+} + 4O^{2-} \rightarrow ZrSiO_4 + CaTiSiO_5 + TiO_2 \quad (2).$$

Titanite and rutile can largely account for the Nb content in zirconolite (Table 2), and columbite also is present in sample 2417 (Fig. 2h). Zirconolite in the garnet-rich cordierite–orthoamphibole gneiss is interpreted to be a relic of igneous in origin, because this mineral has rather limited paragenesis in terrestrial rocks (Gieré 1986, Bayliss *et al.* 1989); rutile and titanite are common metamorphic minerals at Manitouwadge and occur as the breakdown products of zirconolite in the garnet-rich cordierite–orthoamphibole gneiss.

Allanite with a minor amount of Zr (Table 3) in the calc-silicate rock may be directly responsible for the formation of zircon in its replacement assemblages. Gieré (1986) obtained up to 0.58 wt% $ZrO_2$ in allanite associated with zirconolite. Pan & Fleet (1992) reported that allanite in calc-silicate rocks at Manitouwadge is part of the main metamorphic assemblage, on the basis of textural relationships. Therefore, the zircon in replacement aggregates after allanite (Fig. 3a) most likely formed during a retrograde event after high-grade metamorphism. However, zircon younger than 2675 Ma has not been documented at Manitouwadge.

*Formation of metamorphic monazite*

In the garnet-rich cordierite–orthoamphibole gneiss, the prismatic grains of monazite have a Th-rich composition that is consistent with an igneous origin (*cf.* Burnotte *et al.* 1989, Parrish 1990, Smith & Barreiro 1990). However, there are no ages of 2720 Ma on monazite at Manitouwadge that would confirm the survival

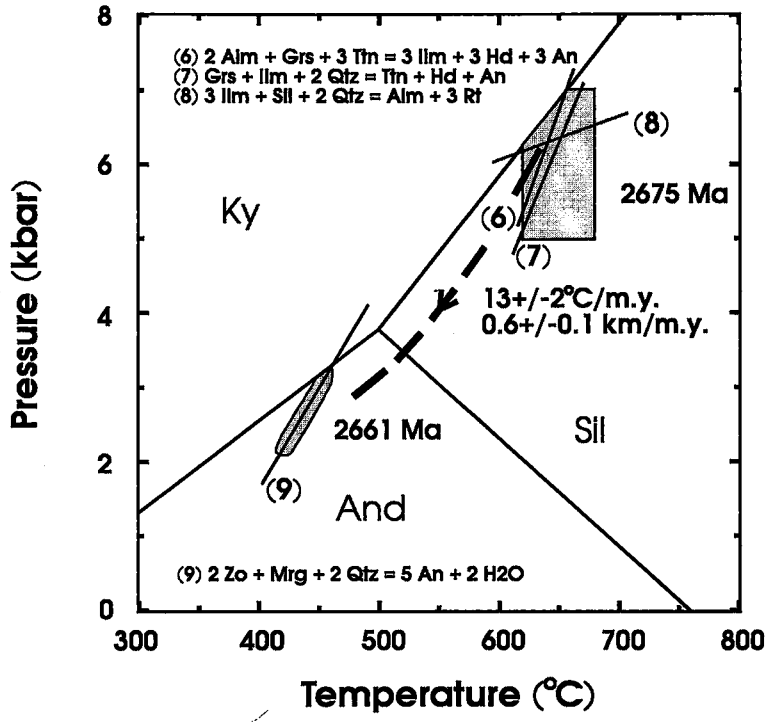


FIG. 4. Metamorphic P–T–t history of the Manitouwadge area. Reactions involving titanite (6 and 7) and rutile (8) are integrated with the U–Pb ages of zircon and monazite [2675 Ma: Davis *et al.* (1994) Schandl *et al.* (1995)] for the peak regional metamorphism. Reaction 9 involving zoisite (epidote) is integrated with the U–Pb age of monazite [2661 Ma: Davis *et al.* (1994)] for the retrograde event. Reactions (6) and (7) are calculated using mineral compositions of sample 11303 (data available upon request from the author) and the TWEEQU method of Berman (1991). Reactions (8) and (9) are from Petersen (1984), and his metamorphic P–T estimates are also shown as shaded areas. Symbols: Alm, almandine; An, anorthite; And, andalusite; Grs, grossular; Hd, hedenbergite; Ilm, ilmenite; Ky, kyanite; Mrg, margarite; Qtz, quartz; Rt, rutile; Sil, sillimanite; Ttn, titanite; and Zo, zoisite.

of igneous monazite after the episode of seafloor hydrothermal alteration and high-grade regional metamorphism. Instead, Davis *et al.* (1994) obtained a U–Pb age of 2675 Ma on Th-rich monazite in muscovite schist of the Geco mine. The Pb closure temperature in monazite (~700°C; Parrish 1990, Heaman & Parrish 1991) is slightly higher than the peak metamorphic temperature at Manitouwadge (650 ± 30°C; Petersen 1984; Fig. 4). Therefore, I contend that Th-rich monazite crystallized during the peak metamorphism, and that the zoning pattern of Th in monazite grains is best explained by Hollister's (1966) Rayleigh fractionation model and the preference of Th for monazite (Parrish 1990). Davis *et al.* (1994) reported 2675 ± 1 Ma for a Th-poor monazite in muscovite schist, also indicative of the crystallization of monazite during the high-grade metamorphism. The common occurrence of anhedral grains of monazite in clusters (Fig. 2f) suggests that this mineral is formed from pre-existing *REE*-rich minerals [allanite?: Bingen *et al.* (1996); apatite during anatexis?: Wolf & London (1995)] during the high-grade metamorphism.

Monazite also crystallized after the high-grade regional metamorphism, as indicated by its presence in replacement assemblages after metamorphic fluorapatite (Fig. 2g), allanite and titanite (Fig. 3). This crystallization of monazite during a retrograde event is supported by the 2661 Ma obtained on Th-poor monazite by Davis *et al.* (1994). Pan *et al.* (1993a) suggested that oriented inclusions of monazite in fluorapatite from the Hemlo gold deposit formed by exsolution processes during late hydrothermal alteration and proposed the following reaction:

$$(Ca_{5-x}REE_x)(P_{3-x}Si_x)O_{12}F + (x-y)Ca^{2+} + 2(x-y)P^{5+} + 6(x-y)O^{2-} \rightarrow (Ca_{5-y}REE_y)(P_{3-y}Si_y)O_{12}F + (x-y)REEPO_4 + (x-y)SiO_2 \quad (3),$$

where $x > y$. The U–Pb monazite dates from the Hemlo gold deposit (2637–2644 Ma: Corfu & Muir 1989) are significantly younger than the peak regional metamorphism at about 2678–2684 Ma. The occurrence of monazite after titanite at Manitouwadge is similar to the replacement of monazite after titanite observed by Pan *et al.* (1993b) and is probably related to the following reactions:

$$(Ca_{1-x}REE_x)(Ti,Al,Fe)SiO_4(O,OH,F) + (x-y)Ca^{2+} + (x-y)(PO_4)^{3-} \rightarrow (Ca_{1-y}REE_y)(Ti,Al,Fe)SiO_4(O,OH,F) + (x-y)REEPO_4 \quad (4),$$

where x > y, or

$$\text{titanite} + (CO_3)^{2-} + (PO_4)^{3-} + F^- + (OH)^- \rightarrow \text{monazite} + \text{quartz} + \text{calcite} + \text{rutile} + \text{epidote} + \text{bastnäsite} + \text{chlorite} \quad (5).$$

In either case, titanite supplied the *REE*, whereas phosphorus may have come from adjacent P-rich minerals (*e.g.*, fluorapatite). Pan *et al.* (1993a, b) showed that areas in fluorapatite and titanite adjacent to monazite contain significantly lower levels of *REE* than unaltered areas, which supports the validity of reactions (3) and (4). A similar process is envisaged for the formation of monazite as a replacement after allanite. Radiation damage may have promoted the replacement processes in both allanite and titanite (Pan *et al.* 1993b).

### *Importance of accessory minerals*

This study shows that the crystallization of zircon and monazite during prograde and retrograde metamorphism at Manitouwadge is largely related to the presence of pre-existing accessory minerals. One can ask whether this observation is applicable to accessory-mineral-rich rocks only? This question can be explored by considering the occurrence of Zr and *REE* in common rock types elsewhere. It is most appropriate to first examine the nature of Zr and *REE* in chlorite-rich rocks (the low-metamorphic-grade equivalent of cordierite–orthoamphibole rocks) associated with other VMS deposits. Pan *et al.* (1994) documented allanite, monazite, zircon and other accessory minerals in chlorite-rich rocks in the footwall of the Mattagami Lake VMS deposit, Quebec, and concluded that some of these accessory minerals are of relict igneous origin, on the basis of textural evidence. Moreover, mass-balance calculations by Pan *et al.* (1994) demonstrated that most of the Zr and *REE* (>70%) in the chlorite-rich rocks resides in the accessory minerals. Similarly, Schandl *et al.* (1991) reported that monazite and xenotime are common accessory minerals in chlorite-rich rocks at Kidd Creek and other VMS deposits of the Superior Province. Therefore, accessory minerals, the major carriers of Zr and *REE*, will largely control the crystallization or recrystallization of zircon and monazite when chlorite-rich rocks are metamorphosed to form cordierite–orthoamphibole rocks.

Accessory minerals are also the major carriers of Zr and *REE* in most common rock types (McLennan 1989). For example, Gromet & Silver (1983) showed that allanite and titanite account for 80–95% of the *REE* in some granitic rocks, whereas major silicates such as plagioclase, alkali feldspar, quartz, and biotite each account for only about 1% or less of the *REE*. Therefore, these major silicate minerals are unlikely major suppliers of Zr and the *REE* for the crystallization of zircon and monazite during metamorphism. In addition, formation of zircon or monazite from the breakdown of Zr–*REE*-poor major silicate minerals would require transport of Zr and the *REE* over significant distances. Zirconium and the *REE* are generally immobile during medium- to high-grade metamorphism, where a prevalent metamorphic fluid is lacking and partial melting is not achieved (McLennan 1989). The diffusion rates of Zr and the *REE* in solid media under metamorphic P–T conditions are most likely exceedingly slow. At Manitouwadge, the preservation of unusual Zr and *REE* characteristics in the garnet-rich cordierite–orthoamphibole gneiss also demonstrates a lack of mobility of these elements during the high-grade regional metamorphism and accompanying anatexis (Pan & Fleet 1995). Formation of zircon and monazite from the breakdown or recrystallization of pre-existing Zr- and *REE*-rich accessory minerals, however, requires only very localized remobilization of Zr and the *REE* (Pan *et al.* 1993a), and therefore is favored (see also Bingen *et al.* 1996). For example, the breakdown of garnet, pyroxenes or amphiboles has been postulated to be responsible for the metamorphic formation of zircon in mafic rocks, in cases where igneous zircon is generally absent (Heaman & Parrish 1991). However, Davidson & van Breemen (1988) demonstrated convincingly that metamorphic zircon in metagabbros of the Grenville Province formed as a replacement of baddeleyite *via* a reaction such as $ZrO_2 + Si^{4+} + (2O^{2-}) \rightarrow ZrSiO_4$.

### *Implications for integration of U–Pb ages with metamorphic P–T estimates*

Although the reactions identified for the crystallization of metamorphic zircon and monazite do not directly involve major silicate minerals (*e.g.*, garnet and biotite) from which metamorphic P–T estimates are commonly obtained, integration of U–Pb data on zircon and monazite with P–T estimates can still be made on the basis of the related accessory minerals. The growth of some accessory minerals (*e.g.*, allanite, fluorapatite, rutile and titanite) in many metamorphic terranes has been well constrained. Moreover, some of these accessory minerals are commonly used in conjunction with

major silicate minerals in geothermobarometry for metamorphic P–T estimates [*e.g.*, rutile: Petersen (1984); titanite: Scott & St-Onge (1995)]. Significant uncertainties, however, exist in directly integrating the U–Pb geochronological results on rutile or titanite to their corresponding P–T estimates in medium- to high-grade metamorphic terranes, because the U–Pb systematics in these accessory minerals are particularly susceptible to disturbance by retrogression or late hydrothermal alteration (Heaman & Parrish 1991, Pan *et al.* 1993b). On the other hand, the paragenetic relationships of minerals used in geothermobarometry with zircon and monazite make an integration between their metamorphic P–T estimates and the robust U–Pb dates of metamorphic zircon and monazite possible. At Manitouwadge, rutile and titanite have been shown to be related to metamorphic zircon, whereas epidote is associated with Th-poor monazite as part of the retrograde metamorphism. Figure 4 illustrates an integration of P–T estimates for the peak regional metamorphism and the retrograde event with the high-precision U–Pb ages of zircon and monazite at Manitouwadge (Davis *et al.* 1994, Schandl *et al.* 1995). This reveals a cooling rate of over 13 ± 2°C/m.y. and an uplift–erosion rate of at least 0.6 ± 0.1 km/m.y. at Manitouwadge. These results are comparable to the rates of cooling and uplift associated with modern collisional orogenic belts (Koons 1987) and, therefore, support the accretionary model involving arc–trench systems and collisional processes for the tectonic evolution of the Western Superior Province (*cf.* Percival & Williams 1989, Williams *et al.* 1991).

## Conclusions

1) The garnet-rich cordierite–orthoamphibole gneiss and calc-silicate rock from Manitouwadge, Ontario, contain abundant zircon, monazite, xenotime, fluorapatite and titanite, and minor amounts of other exotic accessory minerals.

2) A large number of igneous zircon grains in the garnet-rich cordierite–orthoamphibole gneiss survived seafloor hydrothermal alteration and an upper-amphibolite-facies regional metamorphism. Metamorphic zircon formed largely at the expense of the relict igneous zircon and other pre-existing Zr-rich accessory minerals.

3) Monazite of prismatic habit and Th-rich composition most likely crystallized during the upper-amphibolite-facies metamorphism. Monazite also crystallized during a retrograde event as replacement after metamorphic allanite, fluorapatite and titanite.

4) The U–Pb dates of metamorphic zircon and monazite can be integrated with metamorphic P–T estimates based on their related accessory minerals to provide important insights into the tectonic evolution of metamorphic terranes.

## Acknowledgements

I thank K.M. Ansdell, E. Schandl, H. Stowell and N. Wodicka for constructive criticism and helpful suggestions, R.F. Martin for editorial assistance, M.E. Fleet and N.D. MacRae for provision of samples, T. Bonli and B. Morgan for analytical assistance, and N. Chen for the preparation of Figure 1. This study was supported by an NSERC research grant.

## References

Alldrick, D.J. (1974): *Petrography and Geochemistry of the Cordierite–Gedrite Gneiss, Manitouwadge, Ontario.* B.Sc. thesis, Univ. Western Ontario, London, Ontario.

Ansdell, K.M. & Kyser, T.K. (1991): Plutonism, deformation, and metamorphism in the Proterozoic Flin Flon greenstone belt, Canada: limits on timing provided by the single-zircon Pb-evaporation technique. *Geology* **19**, 518-521.

Bayliss, P., Mazzi, F., Munno, R. & White, T.J. (1989): Mineral nomenclature: zirconolite. *Mineral. Mag.* **53**, 565-569.

Berman, R.G. (1991): Thermobarometry using multi-equilibrium calculations: a new technique with petrological applications. *Can. Mineral.* **29**, 833-855.

Bingen, B., Demaiffe, D. & Hertogen, J. (1996): Redistribution of rare earth elements, thorium, and uranium over accessory minerals in the course of amphibolite to granulite facies metamorphism: the role of apatite and monazite in orthogneisses from southwestern Norway. *Geochim. Cosmochim. Acta* **60**, 1341-1354.

Burnotte, E., Pirard, E. & Michel, G. (1989): Genesis of gray monazites: evidence from the Paleozoic of Belgium. *Econ. Geol.* **84**, 1417-1429.

Chakoumakos, B.C., Murakami, T., Lumpkin, G.R. & Ewing, R.C. (1987): Alpha-decay induced fracturing in zircon: the transition from the crystalline to the metamict state. *Science* **236**, 1556-1559.

Corfu, F. & Muir, T.L. (1989): The Hemlo – Heron Bay greenstone belt and Hemlo Au–Mo deposit, Superior Province, Ontario, Canada. 2. Timing of metamorphism, alteration and Au mineralization from titanite, rutile and monazite U–Pb geochronology. *Chem. Geol.* **79**, 201-223.

Davidson, A. & Van Breemen, O. (1988): Baddeleyite–zircon relationships in coronitic metagabbro, Grenville Province, Ontario: implications for geochronology. *Contrib. Mineral. Petrol.* **100**, 291-299.

Davis, D.W., Schandl, E.S. & Wasteneys, H.A. (1994): U–Pb dating of minerals in alteration halos of Superior Province massive sulphide deposits: syngenesis vs. metamorphism. *Contrib. Mineral. Petrol.* **115**, 427-437.

FEDOROWICH, J.S., JAIN, J.C., KERRICH, R. & SOPUCK, V. (1995): Trace-element analysis of garnet by laser-ablation microprobe ICP–MS. *Can. Mineral.* 33, 469-480.

FRIESEN, R.G., PIERCE, G.A. & WEEKS, R.M. (1982): Geology of the Geco base metal deposit. *In* Precambrian Sulphide Deposits (R.W. Hutchinson, C.D. Spence & J.M. Franklin, eds.). *Geol. Assoc. Can., Spec. Pap.* **25**, 343-363.

GIERÉ, R. (1986): Zirconolite, allanite and hoegbomite in a marble skarn from the Bergell contact aureole: implications for mobility of Ti, Zr and *REE*. *Contrib. Mineral. Petrol.* **93**, 459-470.

GROMET, L.P. (1991): Direct dating of deformational fabrics. *In* Applications of Radiogenic Isotope Systems to Problems in Geology (L. Heaman & J.N. Ludden, eds.). *Mineral. Assoc. Can., Short-Course Handbook* **19**, 167-189.

_____ & SILVER, L.T. (1983): Rare earth element distribution among minerals in a granodiorite and their petrogenetic implications. *Geochim. Cosmochim. Acta* **47**, 925-939.

GUPTA, L.N. & JOHANNES, W. (1985): Effect of metamorphic and partial melting of host rocks on zircons. *J. Metamorphic Geol.* **3**, 311-323.

HEAMAN, L. & PARRISH, R. (1991): U–Pb geochronology of accessory minerals. *In* Applications of Radiogenic Isotope Systems to Problems in Geology (L. Heaman & J.N. Ludden, eds.). *Mineral. Assoc. Can., Short-Course Handbook* **19**, 59-102.

HOLLISTER, L.S. (1966): Garnet zoning: an interpretation based on the Rayleigh fractionation model. *Science* **154**, 1647-1651.

JAMES, R.S., GRIEVE, R.A.F. & PAUK, L. (1978): The petrology of the cordierite–anthophyllite gneisses and associated mafic and pelitic gneisses at Manitouwadge, Ontario. *Am. J. Sci.* **278**, 41-63.

KOONS, P.O. (1987): Some thermal and mechanical consequences of rapid uplift: an example from the Southern Alps, New Zealand. *Earth Planet. Sci. Lett.* **86**, 307-319.

MCLENNAN, S.M. (1989): Rare earth elements in sedimentary rocks: influence of provenance and sedimentary processes. *Rev. Mineral.* **21**, 169-200.

MEZGER, K., HANSON, G.N. & BOHLEN, S.R. (1989): U–Pb systematics of garnet: dating the growth of garnet in the Late Archean Pikwitonei granulite domain at Cauchon and Natawahuan Lakes, Manitoba, Canada. *Contrib. Mineral. Petrol.* **101**, 136-148.

PAN, YUANMING & FLEET, M.E. (1990): Halogen-rich allanite from the White River gold occurrence, Hemlo area, Ontario. *Can. Mineral.* **28**, 67-75.

_____ & _____ (1992): Mineralogy and genesis of calc-silicates associated with Archean volcanogenic massive sulphide deposits at the Manitouwadge mining camp, Ontario. *Can. J. Earth Sci.* **29**, 1375-1388.

_____ & _____ (1993): Rare earth minerals in some Canadian precious-metal and massive sulfide deposits. *In* Rare Earth Minerals: Crystal Chemistry, Origin and Ore Deposits. Mineralogical Society, London, U.K. (abstr.).

_____ & _____ (1995): Geochemistry and origin of cordierite–orthoamphibole gneisses and associated rocks at an Archean volcanogenic massive sulphide camp: Manitouwadge, Ontario, Canada. *Precamb. Res.* **74**, 73-89.

_____, _____ & BARNETT, R.L. (1994): Rare-earth mineralogy and geochemistry at the Mattagami volcanogenic massive sulfide deposit, Quebec. *Can. Mineral.* **32**, 133-147.

_____, _____ & MACRAE, N. (1993a): Oriented monazite inclusions in apatite porphyroblasts from the Hemlo gold deposit, Ontario, Canada. *Mineral. Mag.* **57**, 697-707.

_____, _____ & _____ (1993b): Late alteration in titanite ($CaTiSiO_5$): redistribution and remobilization of rare earth elements and implications for U/Pb and Th/Pb geochronology and nuclear waste disposal. *Geochim. Cosmochim. Acta* **57**, 355-367.

PARRISH, R.R. (1990): U–Pb dating of monazite and its application to geological problems. *Can. J. Earth Sci.* **27**, 1431-1450.

PERCIVAL, J.A. & WILLIAMS, H.R. (1989): The Late Archean Quetico accretionary complex, Superior Province, Canada. *Geology* **17**, 23-25.

PETERSEN, E.U. (1984): *Metamorphism and Geochemistry of the Geco Massive Sulfide Deposit and its Enclosing Wall-Rocks.* Ph.D. thesis, Univ. Michigan, Ann Arbor, Michigan.

PIDGEON, R.T. (1992): Recrystallization of oscillatory zoned zircon – some geochronological and petrological implications. *Contrib. Mineral. Petrol.* **110**, 463-472.

POLDERVAART, A. (1956): Zircons in rocks. 2. Igneous rocks. *Am. J. Sci.* **254**, 521-554.

ROBINSON, P.C. (1979): *Geology and Evolution of the Manitouwadge Migmatite Belt, Ontario, Canada.* Ph.D. thesis, Univ. Western Ontario, London, Ontario.

ROEDER, P.L. (1985): Electron-microprobe analysis of minerals for rare-earth elements: use of calculated peak-overlap corrections. *Can. Mineral.* **23**, 263-271.

SCHANDL, E.S., DAVIS, D.W., GORTON, M.P. & WASTENEYS, H.A. (1991): Geochronology of hydrothermal alteration around volcanic-hosted massive sulphide deposits in the Superior Province. *Ontario Geol. Surv., Misc. Pap.* **156**, 105-120.

_____, GORTON, M.P. & WASTENEYS, H.A. (1995): Rare earth element geochemistry of the metamorphosed volcanogenic massive sulfide deposits of the Manitouwadge mining camp, Superior Province, Canada: a potential exploration tool? *Econ. Geol.* **90**, 1217-1236.

SCHUMACHER, J.C. & ROBINSON, P. (1987): Mineral chemistry and metasomatic growth of aluminous enclaves in gedrite–cordierite gneiss from southwestern New Hampshire, USA. *J. Petrol.* 28, 1033-1073.

SCOTT, D.J. & ST-ONGE, M.R. (1995): Constraints on Pb closure temperature in titanite based on rocks from the Ungava orogen, Canada: implications for U–Pb geochronology and P–T–t path determinations. *Geology* **23**, 1123-1126.

SMITH, H.A. & BARREIRO, B. (1990): Monazite U–Pb dating of staurolite grade metamorphism in pelitic schists. *Contrib. Mineral. Petrol.* **105**, 602-615.

STEVENSON, R.K. & MARTIN, R.F. (1986): Implications of the presence of amazonite in the Broken Hill and Geco metamorphosed sulfide deposits. *Can. Mineral.* **24**, 729-745.

VAVRA, G., GEBAUER, D., SCHMID, R. & COMPSTON, W. (1996): Multiple zircon growth and recrystallization during polyphase Late Carboniferous to Triassic metamorphism in granulites of Ivrea Zone (southern Alps): an ion microprobe (SHRIMP) study. *Contrib. Mineral. Petrol.* **122**, 337-358.

WILLIAMS, H.R., STOTT, G.M., HEATHER, K.B., MUIR, T.L. & SAGE, R.P. (1991): Wawa Subprovince. *In* Geology of Ontario (P.C. Thurston, H.R. Williams, R.H. Sutcliffe & G.M. Scott, eds.). *Ontario Geol. Surv. Spec. Vol.* **4**, 485-542.

WOLF, M.B. & LONDON, D. (1995): Incongruent dissolution of *REE*- and Sr-rich apatite in peraluminous granitic liquids: differential apatite, monazite, and xenotime solubilities during anatexis. *Am. Mineral.* **80**, 765-775.

ZALESKI, E. & PETERSON, V.L. (1996): Depositional setting and deformation of massive sulfide deposits, iron-formation, and associated alteration in the Manitouwadge greenstone belt, Superior Province, Ontario. *Econ. Geol.* **90**, 2244-2261.

_____, _____ & VAN BREEMEN, O. (1994): Geological, geochemical, and age constraints on base metal mineralization in the Manitouwadge greenstone belt, northwestern Ontario. *Geol. Surv. Can., Current Res.* **1994-C**, 225-235.

_____, _____ & _____ (1995): Geological and age relationships of the margins of the Manitouwadge greenstone belt and the Wawa–Quetico subprovince boundary, northwestern Ontario. *Geol. Surv. Can., Current Res.* **1995-C**, 35-44.

*Received April 17, 1996, revise manuscript accepted October 28, 1996.*